ISBN: 978-3-95450-247-9 ISSN: 2673-5490 doi: 10.18429/JACoW-IPAC2024-WEPR28

RADIATION LOAD STUDIES FOR THE PROTON TARGET AREA OF A MULTI-TeV MUON COLLIDER*

J. Mańczak†, C. Ahdida, L. Bottura, M. Calviani, D. Calzolari, R. Franqueira Ximenes, A. Frasca, A. Lechner, F. J. Saura Esteban, D. Schulte, CERN, Geneva, Switzerland
C. Rogers, ISIS Neutron and Muon Source, STFC, Oxfordshire, United Kingdom
A. Portone, Fusion for Energy, Barcelona, Spain

Abstract

Muon production in the multi-TeV muon collider studied by the International Muon Collider Collaboration is planned to be performed with a high-power proton beam interacting with a fixed target. The confinement of the emerging pions and muons requires very strong magnetic fields achievable only by superconducting solenoids, which are sensitive to heat load and long-term radiation damage. The latter concerns the ionising dose in insulation, as well as the displacement damage in the superconductor. Furthermore, the fraction of the primary beam passing through the target unimpeded poses a need for an extraction channel. In this study, we use the FLUKA Monte Carlo code to assess the radiation load to the front-end solenoids, and we explore a possible spent proton beam extraction scenario.

INTRODUCTION

The International Muon Collider Collaboration (IMCC) is exploring the feasibility of a multi-TeV muon collider facility [1–3]. One of the technical challenges is posed by the muon production through the interaction of a high-power proton beam with a target. Proton interactions generate secondary pions, which are captured by high-field solenoids and eventually decay into muons. The IMCC aims to develop an integrated front-end design, which employs suitable engineering solutions while optimizing the delivery of a high-intensity and high-quality muon beam to reach the desired luminosities. The presently considered proton beam parameters are summarized in Table 1, with proton energy of 5 GeV and a beam power of 2 MW. The baseline target assembly consists of an 80 cm-long isostatic graphite rod (1.8 g/cm^3), with a diameter of 30 mm, which is housed in a titanium vessel filled with helium gas [4].The latter prevents sublimation of the graphite due to the high temperatures by facilitating the heat dissipation from the target rod.

Considering the MW-scale drive beam power, massive radiation shielding elements are needed in the target area for equipment protection. The solenoids near the production target are exposed to the secondary particle showers generated by inelastic collision products in the graphite rod. Dedicated radiation absorbers need to be embedded inside the magnet aperture in order to attenuate the showers before they reach the coils. The shielding must prevent beam-induced magnet quenches, reduce the thermal load to the cryogenic system, and prevent magnet failures due to the cumulative radiation damage. The latter concerns the ionizing dose in organic materials (e.g. insulation, spacers) and atomic displacements in superconductors. Radiation studies for muon production front-ends have been carried out previously for neutrino factories, as well as for muon colliders within the US-Muon Accelerator Program (MAP) [5–8].

Table 1: Proton Driver Beam Parameters

Beam power [MW]	2	Pulse frequency [Hz]	5
Beam energy [GeV]	5	Beam size $\sigma_{x,y}$ [mm]	5

A new pion-capture solenoid configuration, based on high-temperature superconductors (HTS) without normal-conducting inserts, has been developed within the IMCC, with a peak field of 20 T [9]. In this paper, we present power deposition and radiation damage studies for the proposed target and front-end design. In particular, we quantify the necessary arrangement of shielding inserts that protect the HTS magnets. Furthermore, we discuss the extraction of spent protons, which pass the target without undergoing inelastic collisions. These protons have to be safely disposed off on a dedicated beam dump without causing damage to front-end equipment. We quantify the required dimensions for a possible proton extraction channel. All studies were carried out with the FLUKA Monte Carlo code [10–12].

FRONT-END LAYOUT AND MUON YIELD

The FLUKA simulation geometry used for the evaluation of the muon yield and radiation load to equipment is shown in Fig. 1. This simplified model includes only the elements which are relevant for the study. The front-end features a sequence of identical-aperture HTS solenoids, which have a total length of about 18 m. The solenoids embed a radiation shielding made of helium gas-cooled tungsten segments. The shielding has a tapered aperture downstream of the target in order to confine the secondary pions and muons. The tapered aperture follows a parabolic shape, with a radius of 17.8 cm at the production target and a radius of 40 cm after 17.5 m. The solenoid layout is still a subject of optimisation; the presented configuration is meant provide the desired magnetic field profile, without fully taking into account engineering constraints. The B-field is tapered from 20 T to 1.5 T at the entrance of the chicane. Table 2 summarizes the assumed radial build of the shielding and solenoid at the

* Funded by the European Union (EU). Views and opinions expressed are however those of the author(s) only and do not necessarily reflect those of the EU or European Research Executive Agency (REA). Neither the EU nor the REA can be held responsible for them.
† jerzy.mikolaj.manczak@cern.ch

ISBN: 978-3-95450-247-9 ISSN: 2673-5490 doi: 10.18429/JACoW-IPAC2024-WEPR28

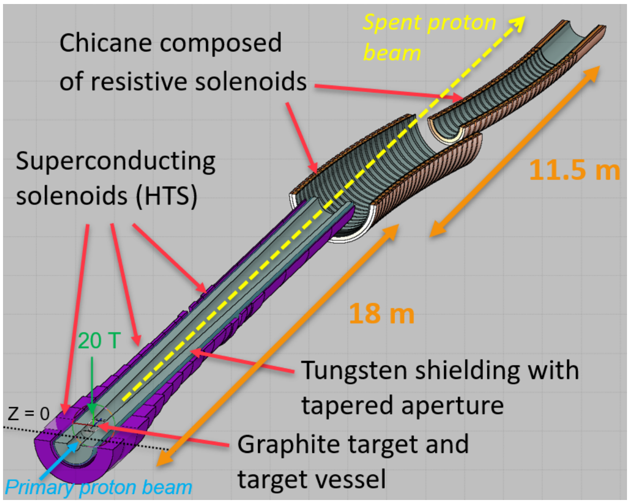

Figure 1: FLUKA model for radiation studies.

Table 2: Radial Build around Target for the Radiation Studies

	r	r_{outer}
Target rod (graphite)	1.5 cm	1.5 cm
Gas (He)	15 cm	16.5 cm
Target vessel	0.5 cm	17.0 cm
Clearance to shielding	0.8 cm	17.8 cm
Radiation shielding	39.7–59.7 cm	57.5–77.5 cm
Supports, therm. insul.	7.5 cm	65–85 cm
Solenoid (HTS-based)	48 cm	113–133 cm

location of the target. Different shielding thicknesses were considered in the FLUKA studies, ranging from ~40 cm to ~60 cm. In order to thermalize and capture neutrons, the shielding was assumed to include a layer of water (2 cm) and boron carbide (0.5 cm) close to the outer shielding boundary. The model also assumes a gap between the shielding and the inner magnet bore in order to accommodate a thermal shielding and supports.

A chicane made of resistive solenoids is placed right after the tapered region to filter out the high-momentum particles. At the same time, the design of the chicane has to accommodate space for the extraction channel of the spent primary protons. Figure 1 shows an example chicane design, which was first proposed in [13] and attempts to fulfil both of the above-mentioned conditions. The magnetic field strength is optimised to keep 1.5 T across the chicane's central axis. The proton extraction channel is located in the middle of the chicane (dashed yellow line), using solenoids of different aperture (radius of 100 cm and 40 cm). The central axes of the first and last solenoids have a lateral offset of 160 cm. The field is too weak to significantly affect the protons with energies of a few GeV, but it is enough to guide the muons and pions further downstream. Figure 2 presents the momentum distribution of muons and pions entering and leaving the chicane, as simulated with FLUKA. The simulation predicts a pion/muon yield (per primary proton) of 0.17 $\pi^+ + \mu^+$ and 0.12 $\pi^- + \mu^-$ at the end of the chicane.

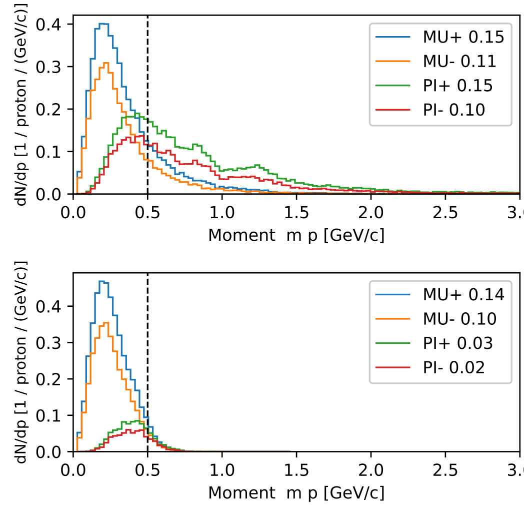

Figure 2: Momentum distribution of pions and muons entering (top) and leaving (bottom) the chicane. The chicane suppresses the higher-moment component above ~0.5 GeV/c (dashed line). The numbers in the legend correspond to the pion/muon yield per primary proton.

POWER DEPOSITION

Table 3 summarizes the power deposition in the target assembly, shielding, HTS solenoids and chicane for the smallest shielding thickness specified in Table 2 (~40 cm). The power of the extracted protons is calculated within 30 cm radius around the center of the proton distribution (see last section). The shielding dissipates almost half (45%) of the initial proton beam power, while only 7.4% is deposited in the target rod and vessel. The most exposed HTS-based solenoid absorbs about 0.08% of the power, which corresponds to 1.7 kW. In total, the power load on superconducting solenoids is less than 5 kW, which is considered acceptable for the heat evacuation from the cold mass. A large fraction of the initial beam power escapes from the tapered region (about 42% or 850 kW). Out of this power, only 22 kW is converted into useful pions and muons, while 402 kW is carried by spent protons, which have to be extracted since the energy is still concentrated in a relatively focused beam. About 95 kW is deposited in the chicane, while the rest is dissipated elsewhere. The most loaded resistive solenoid in

Table 3: Power Deposition in the Target Area

	Absolute	Relative
Target	112 kW	5.6%
Target vessel	35 kW	1.8%
Rad. shielding	894 kW	44.7%
Most loaded HTS solenoid	1.7 kW	0.08%
Other HTS solenoids (sum)	2.9 kW	0.15%
Most loaded chicane magnet	24.5 kW	1.2%
Rest of the chicane structure	70.8 kW	3.5%
Protons extracted (R<30 cm)	402 kW	20.1%
Muons/pions captured	21.9 kW	1.2%
Elsewhere	296 kW	14.8%

ISBN: 978-3-95450-247-9 ISSN: 2673-5490 doi: 10.18429/JACoW-IPAC2024-WEPR28

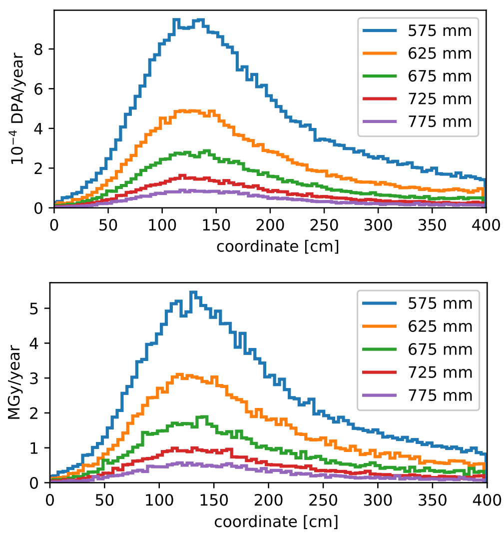

Figure 3: Maximum ionizing dose and DPA (per year) along the HTS target solenoids for various shielding thicknesses. The labels give the outer radius of the shielding. The graphite target extends from 40 cm to 120 cm.

the chicane absorbs 25 kW, requiring an improved shielding design. Furthermore, 5% of the initial power is spent in nuclear collisions and 2% escapes in the form of neutrinos (not included in the table).

CUMULATIVE RADIATION DAMAGE IN HTS SOLENOIDS

Figure 3 shows the maximum ionizing dose and DPA in the HTS coils along the beam direction. The results are given for one operational year, assuming a run time of $1.2{\times}10^7$ s (equivalent to ≈140 days with 100% machine availability). The DPA calculation is based on the Norget-Torrens-Robinson (NRT)-model [14] in FLUKA, with the material-specific damage threshold energies taken from Ref. [15]. The different curves correspond to different tungsten shielding thicknesses and coil apertures (see Table 2). The highest dose and DPA values can be observed near the target position, due to showers induced by secondary protons, neutrons and pions, which are lost on the inner shielding aperture.

The studies indicate that a shielding thickness of about 40 cm (inner magnet radius of 65 cm) results in a peak dose of about 5 MGy/year, and a displacement damage of about 10^{-3} DPA/year. Increasing the shielding to ~60 cm (inner magnet radius of 85 cm) reduces the dose and DPA in the coils by about factor of ten. A dose of 5 MGy/year could possibly be acceptable for insulation materials if one assumes 10 years of operation, but leaves no safety margin if common materials like Kapton are used [16]. The maximum allowed DPA in the coils per year of operation needs to be further assessed. Previous irradiation experiments showed that the critical temperature of different HTS samples start to be affected above 10^{-3} DPA [17]. However, the magnet performance can possibly be restored by annealing [18]. Assuming 10 years of operation, the inner radius of the target

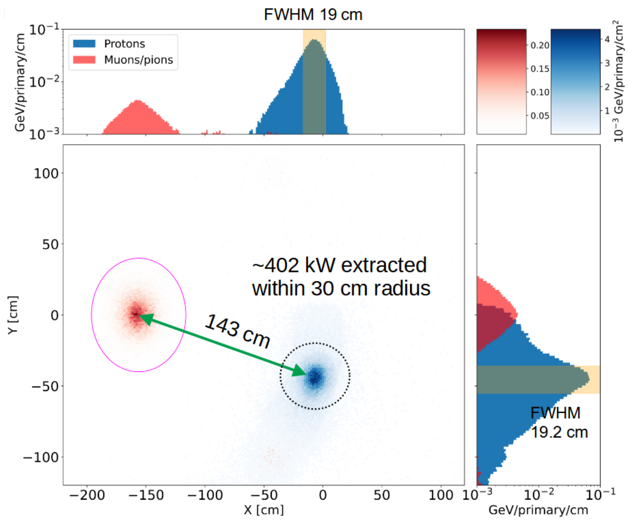

Figure 4: Energy-weighted distribution of particles crossing the transverse plane at the end of the chicane. The magenta circle represents the chicane aperture.

solenoid might need to be in the range from 65 cm (assuming optimistically a full recovery of properties due to annealing) and 85 cm (no effect of annealing).

EXTRACTION OF SPENT PROTON BEAM

The spent protons would give rise to a high power deposition density in the chicane if they would not be extracted. In the following, we quantify the required size of an extraction channel in the chicane, as illustrated in Fig. 1, in order to steer the protons onto an external beam dump. After the extraction point, there needs to be sufficient space for beam-guiding equipment and the beam dump placement. The spatial distribution of the particles crossing the plane parallel to the end of the chicane is shown in Fig. 4. The red distribution corresponds to pions and muons, which follow the chicane, whereas the blue distribution gives the protons exiting from the gap between the solenoids. Both distributions have been weighted with the energy of the particles to highlight the area where the most energy is extracted. The spent proton beam is slightly bent downwards due to the effect of the magnetic field in the chicane. Most of the energy carried out by the protons is accumulated within a spot of about 30 cm diameter, which is well separated (~140 cm) from the muon/pion distribution.

CONCLUSIONS

The paper investigated the shielding requirements for protecting HTS solenoids in a proton-driven 2 MW target facility of a muon collider. The displacement damage in the superconductor is found to be one of the main factors for the shielding design, but the actual shielding requirements will depend on the recovery of properties through annealing. The studies further showed that an extraction channel for the spent proton beam in the chicane needs to have a diameter of about 30 cm in order to accommodate the most energetic protons.

ISBN: 978-3-95450-247-9 ISSN: 2673-5490 doi: 10.18429/JACoW-IPAC2024-WEPR28

REFERENCES

[1] D. Schulte, "The International Muon Collider Collaboration," in *Proc. IPAC'21*, Campinas, Brazil, May 2021, pp. 3792–3795. doi:10.18429/JACoW-IPAC2021-THPAB017

[2] D. Schulte, "The Muon Collider," in *Proc. IPAC'22*, Bangkok, Thailand, 2022, pp. 821–826. doi:10.18429/JACoW-IPAC2022-TUIZSP2

[3] C. Accettura *et al.*, "Towards a muon collider," *Eur. Phys. J. C*, vol. 83, no. 9, p. 864, 2023, [Erratum: Eur.Phys.J.C 84, 36 (2024)]. doi:10.1140/epjc/s10052-023-11889-x

[4] F. J. S. Esteban *et al.*, "Muon Collider Graphite Target Studies and Demonstrator Layout Possibilities at CERN," in *Proc. IPAC'22*, Bangkok, Thailand, 2022, pp. 2895–2898. doi:10.18429/JACoW-IPAC2022-THPOTK052

[5] N. V. Mokhov, "Particle Production and Radiation Environment at a Neutrino Factory Target Station," in *Proc. PAC'01*, Chicago, IL, USA, Jun. 2001, pp. 745–747. https://jacow.org/p01/papers/FOAC010.pdf

[6] J. J. Back *et al.*, "Particle Production Simulations for the Neutrino Factory Target," in *Proc. IPAC'11*, San Sebastian, Spain, 2011, pp. 835–837. https://jacow.org/IPAC2011/papers/MOPZ008.pdf

[7] J. J. Back, C. Densham, R. Edgecock, and G. Prior, "Particle production and energy deposition studies for the neutrino factory target station," *Phys. Rev. Spec. Top. Accel. Beams*, vol. 16, p. 021 001, 2 2013. doi:10.1103/PhysRevSTAB.16.021001

[8] H. G. Kirk *et al.*, "Beam-power Deposition in a 4-MW Target Station for a Muon Collider or a Neutrino Factory," in *Proc. IPAC'11*, San Sebastian, Spain, 2011, pp. 1653–1655. https://jacow.org/IPAC2011/papers/TUPS054.pdf

[9] C. Accettura *et al.*, "Conceptual design of a target and capture channel for a muon collider," *IEEE Trans. Appl. Supercond.*, vol. 34, no. 5, pp. 1–5, 2024. doi:10.1109/TASC.2024.3368387

[10] CERN, *Fluka website*, https://fluka.cern/.

[11] G. Battistoni, T. Boehlen, F. Cerutti, P. W. Chin, L. S. Esposito, A. Fassò, *et al.*, "Overview of the FLUKA code," *Ann. Nucl. Energy*, vol. 82, 10–18. 9 p, 2015. doi:10.1016/j.anucene.2014.11.007

[12] C. Ahdida, D. Bozzato, D. Calzolari, F. Cerutti, N. Charitonidis, A. Cimmino, *et al.*, "New Capabilities of the FLUKA Multi-Purpose Code," *Front. Phys.*, vol. 9, 2022. doi:10.3389/fphy.2021.788253

[13] C. Rogers, *Muon Chicane*, Presented at the Muon Target Meeting (19/10/2023), 2023.

[14] M. Norgett, M. Robinson, and I. Torrens, "A proposed method of calculating displacement dose rates," *Nucl. Eng. Des.*, vol. 33, no. 1, pp. 50–54, 1975. doi:10.1016/0029-5493(75)90035-7

[15] R. MacFarlane and A. Kahler, "Methods for processing endf/b-vii with njoy," *Nucl. Data Sheets*, vol. 111, no. 12, pp. 2739–2890, 2010, Nuclear Reaction Data. doi:10.1016/j.nds.2010.11.001

[16] L. Bottura and P. Fessia, "What could stop us and when," 2014. doi:10.5170/CERN-2014-006.35

[17] M. Eisterer, "Radiation effects in superconductors," presented at the IMCC Annual Collaboration Meeting 2022, CERN, Geneva, Switzerland, https://indico.cern.ch/event/1250075, 2022.

[18] R. Unterrainer, D. X. Fischer, A. Lorenz, and M. Eisterer, "Recovering the performance of irradiated high-temperature superconductors for use in fusion magnets," *Supercond. Sci. Technol.*, vol. 35, no. 4, 04LT01, 2022. doi:10.1088/1361-6668/ac4636